

## ADVANCED PROPELLER AERODYNAMIC ANALYSES

Lawrence J. Bober  
National Aeronautics and Space Administration  
Lewis Research Center

### SUMMARY

Three advanced analysis methods for predicting the aerodynamic performance of propellers are presented. Two of these analyses are lifting-line methods, and the third is a lifting-surface method. The approach used in each of the methods is described, and the capabilities are presented.

### INTRODUCTION

Increased concern over fuel cost and availability have fostered renewed interest in propellers for aircraft propulsion because of the propeller's inherent high efficiency compared with a turbofan. The quest for improved efficiency and lower noise at high subsonic flight speeds at 30 000 feet or more has forced propellers away from conventional designs toward the type shown in the previous paper. The combination of high flight speed and high rotational speed has resulted in propellers with a large number of highly swept blades having significant cascade effects in the inboard region of the blades. Carefully contoured nacelles contribute to the already complex flow field associated with the propeller. These radically different geometries and the complex flow fields they cause cannot be adequately analyzed using conventional aerodynamic performance analyses. To overcome the shortcomings of established approaches to propeller performance predictions, advanced propeller aerodynamic analyses are being developed as part of NASA's Advanced Turboprop Program.

This paper will discuss three advanced analyses currently under development. Two are lifting-line analyses in which each blade is represented by a single line of vorticity. The third is a lifting-surface analysis in which each blade is represented as a solid surface. Although these analyses were developed for the kinds of propellers described in the previous paper, they have features that are applicable to both low and high-speed general-aviation propellers. Before discussing the advanced analyses, an established approach to propeller performance prediction will be discussed.

### ESTABLISHED APPROACH

In a velocity potential solution for the flow around a propeller, the non-uniform spanwise loading on the blades causes a sheet of vorticity to extend

downstream to infinity as shown in figure 1. This vortex wake is shown as a finite number of filaments, but could more accurately be represented as an infinite number of vortex filaments. The vortex wake is important in propeller performance prediction since it causes an induced velocity at the propeller, thereby changing the local blade angle of attack.

The important features of this established approach are summarized in figure 1. Calculation of the induced flow in this approach is based on the work done by Goldstein (ref. 1) about 50 years ago. Because of the limited computing capability at that time, Goldstein used a very simplified model so that he could obtain an analytical solution for the induced velocity at the propeller due to the wake. He assumed that the shape of the wake was a rigid helix which was known to correspond to a lightly loaded propeller with optimum distribution of loading. To visualize a rigid helical wake, consider a plane normal to the axis of revolution of the propeller. The intersection of this plane with the rigid helical wake is a straight line. Another feature of this wake shape is that the pitch of the helix does not change with axial location. (This wake is shown in fig. 1.) Goldstein published results for single rotation propellers (ref. 1), and Theodorsen obtained results for coaxial counterrotating propellers using an electrical analogy (ref. 2). The induced velocities obtained from the Goldstein and Theodorsen results are strictly correct only for straight propeller blades. Also their original works contained no provisions for a nacelle since the vorticity extended to the axis of the propeller. These results form the basis of a procedure which has been refined over the years and has become an established approach to propeller performance analysis.

This procedure is implemented using a strip analysis in which the flow conditions are determined at one radial location at a time. For each strip the induced velocity is determined from Goldstein's or Theodorsen's results. The effect of the nacelle is taken into account in an approximate manner by assuming that at each strip the induced velocity is the same as for the entire propeller operating at the same velocity that exists at that strip. The total velocity is then the vector sum of the induced velocity, the local velocity for the isolated nacelle, and the rotational velocity. The flow velocity and the blade geometry determine the local blade angle of attack, which allows the determination of the lift and drag coefficients from isolated airfoil data. Sweep is taken into account through the cosine rule (ref. 3). These forces are resolved into thrust and torque components that can be integrated radially to get the propeller thrust, torque, power, and efficiency.

It is important to note that for any operating condition, the effect of the wake is assumed to be the same as for an optimally loaded propeller, even if there is a nacelle and spinner present.

## ADVANCED ANALYSES

### Curved Lifting-Line Analysis

The important features of this analysis are shown in figure 2. The wake is represented by a finite number of helical vortex filaments instead of the con-

tinuous sheet of vorticity used by Goldstein. Each filament has constant pitch, but its location relative to another is arbitrary as shown in figure 2. At any point on the blade, the induced flow due to each wake filament and the lifting line is calculated using the law of Biot-Savart (ref. 3). The total induced flow at any point is then the sum from all these vortices. This analysis is currently restricted to single-rotation propellers. The propeller blades are represented by curved lifting lines of arbitrary shape. The nacelle is restricted to being an infinite cylinder since the wakes cannot contract radially.

The strengths of the wake vortex filaments are related to the spanwise variation of lift on the blade. Thus it is necessary to solve for the blade and wake vortex strengths simultaneously. An important aspect of the solution procedure is the placement of the bound vortex at the quarter chord line and the requirement that the flow be tangent to the mean camber line at the three-quarter chord line. Thus no isolated airfoil data are needed since the lift at any radius can be determined from the vortex strength at the same radius. However, this approach cannot predict the blade drag. This analysis has been developed by Sullivan (ref. 4) at Purdue University under a grant from NASA Lewis Research Center.

An interesting application of this analysis is shown in figure 3, which shows the effect of proplets on propeller performance. A proplet is an aerodynamic device at the tip of the propeller blade similar to winglets, which have been shown to increase the lift-to-drag ratio of wings. If the proplet is properly integrated into the tip flow field, an improvement in performance as shown in figure 3 can be obtained. The plot shows the predicted efficiency as a function of power coefficient for a propeller with and without proplets. The results show an increase in efficiency due to the proplets of about 1 percent at low power and about 3 percent at high power.

The development of this analysis is continuing both at Purdue and at Lewis. Radially varying inflow velocities will be included to better account for the nacelle. A drag prediction procedure using isolated airfoil data will be implemented so that the effect of blade drag can be included.

#### Propeller Nacelle Interaction Analysis

The second advanced lifting-line analysis has more extensive capabilities, which are summarized in figure 4. This analysis was developed by United Technologies Research Center (ref. 5) under contract to Lewis. The wake is represented by a finite number of vortex filaments that are located on stream surfaces so that they conform to the shape of the nacelle. The pitch of these filaments is not constant, and they can contract in both the axial and radial directions. This capability is clearly shown in figure 4 just downstream of the propeller where the wake filaments are displaced radially because of the increasing nacelle diameter. This analysis is capable of analyzing both single and coaxial counterrotating propellers. The blades are represented by lifting lines and can have any arbitrary shape. The nacelle can be any axisymmetric shape.

The solution procedure in this analysis is as follows. First an inviscid solution for the nacelle alone is obtained. The results are used to locate the wake vortex filaments along stream surfaces and to determine the radially varying inflow for the propeller. The induced flow at the propeller due to each wake filament is calculated using the law of Biot-Savart (ref. 3). The total induced velocity at any radial location on a blade is obtained by summing the induced flow from the individual wake filaments and from the lifting lines. The blade lift and drag are determined from two-dimensional airfoil and cascade data. An iteration procedure is required to insure that the wake vortex strengths are consistent with the spanwise load distribution on the blade. A final optional step is to use the blade forces in a circumferentially averaged, viscous, compressible flow calculation.

For a propeller operating at high flight speed or high rotational speed, portions of the blades may be moving at supersonic speeds relative to the undisturbed flow. When this occurs some additional effects (shown in fig. 5) must be considered. In a supersonic flow a disturbance in the flow is felt only in a conical region downstream of the disturbance known as the region of influence. For the propeller shown in figure 5 only the shaded portion of the upper right hand blade is affected by what happens at the tip of the upper left hand blade. Thus, when the induced velocity due to the wake is calculated, it is necessary to limit the region over which each wake filament has an effect. A second consideration is that, when the tip is supersonic, the flow becomes highly three-dimensional near the tip due to the tip Mach cone. This effect is taken into account by applying a correction to the lift determined from isolated airfoil data.

The relative importance of some of these effects is shown in figure 6 where predicted power coefficient is shown as a function of advance ratio. The different curves were obtained using the same computer program but with different options for each curve to isolate certain effects. The configuration analyzed was an eight bladed propeller with  $30^\circ$  of tip sweep (denoted as SR1 in the previous paper). The curve labeled "rigid wake" was obtained using a rigid helical wake without the high-speed effects and is essentially the same as the results that would be obtained with the established approach. For the curve labeled "wake model," the wake filaments were distorted by the nacelle. (The high-speed effects again were not included.) The difference between the two curves is solely due to the different assumed wake shapes. The curve labeled "wake model and high-speed effects" includes the distorted wake and the high-speed effects described in figure 5. The difference between this curve and the "wake model" curve is solely due to the high-speed effects. As expected the largest difference between these two curves occurs at the lowest advance ratio, which corresponds to the highest tip speed. The high-speed effects cause the largest changes to the shape of the curves. From comparisons not shown here, it was found that the shape of the wake model and high speed effects curve agrees with the experimental results, indicating the treatment of these effects in the analysis is qualitatively correct.

Shown in figure 7 are results from the circumferentially averaged, viscous, compressible flow calculation for the configuration shown in figure 6. Each curve in figure 7 represents the radial distribution of circumferentially aver-

aged swirl velocity at that axial location. The uniform spacing of the curves ahead of the propeller indicates no swirl is present in the flow. The distorted curves in the vicinity of the blades indicate that swirl is being introduced into the flow. The uniform spacing of the curves downstream of the blades indicates that the swirl persists in the flow. These results from the viscous calculation are used to check fluid velocities between the blades and downstream of the propeller. If the velocities are too high, large losses due to shock waves can occur. These results also give the pressure and viscous drag on the nacelle in the presence of the propeller. United Technologies Research Center will be doing modifications and applications of this analysis under a follow-on contract.

### Lifting-Surface Analysis

The key features of the three-dimensional, compressible lifting-surface analysis are shown in figure 8. Also shown are partial front and side views of the grid on which the flow calculations are performed. The grid actually extends much further in the radial direction than is shown. The nacelle is required to be axisymmetric so that the flow between each two adjacent blades is the same. Thus it is only necessary to solve for the flow between two blades. The flow is required to be tangent to all solid surfaces and beyond the blade tips is assumed to be periodic. The equations of motion in finite-difference form, are solved at discrete points in the grid. The equations that are solved are the three-dimensional, unsteady, Euler equations, which govern the inviscid flow of a compressible fluid and can accurately represent the pressure variation caused by shock waves and the work done by the propeller on the fluid. The equations are solved by marching in time using an implicit finite-difference method until a steady state is reached. No wake modeling or two-dimensional airfoil data are required. Viscous effects, however, are not included. This analysis was developed by Kutler of NASA Ames Research Center and Chaussee of Nielsen Engineering and Research and is described in reference 6.

Results from this lifting surface analysis are shown in figure 9 for an eight bladed propeller having  $30^\circ$  of sweep at the blade tips. The plots show the distribution of static pressure coefficient on the suction and pressure surfaces of the blades at three spanwise locations from near the hub to near the tip. The most significant feature of these results is the predicted shock wave along the entire span of the blade. At the conditions for which these results were obtained, experimental data also indicate compressibility losses. The detailed spanwise and chordwise distribution of loading predicted by this code is important for improved propeller designs from acoustic and structural standpoints. Development of this code is continuing at Lewis.

### FUTURE PLANS

The development of these advanced analyses will continue. Initial comparisons of the analytical results from all these advanced methods with performance data have shown qualitative agreement (ref. 7). However, performance data cannot substantiate the details of the flow as predicted by the analyses. Thus an experimental program is planned for the Lewis 8x6 foot wind tunnel in 1980 to

provide detailed data for verifying these analyses. A laser velocimeter system (fig. 10) will be used to make these measurements since this type of system does not introduce hardware which might disturb the flow. This experimental program will define the details of the flow around the blades and upstream and downstream of the propeller. These results will pinpoint any deficiencies in the analyses so that quantitative, as well as qualitative, agreement can be obtained.

#### CONCLUDING REMARKS

Three advanced analyses for predicting propeller aerodynamic performance have been presented. The analytical approaches as well as the capabilities of these analyses have been described. Two of these analyses use a lifting-line representation for the propeller blades, and the third uses a lifting-surface representation. The detailed flow-field measurements to be made in the near future will provide data for validating the analyses, making them available as analytical tools for designing improved propellers.

#### REFERENCES

1. Goldstein, S.: On the Vortex Theory of Screw Propellers. Proc. Roy. Soc., (London), vol. 123, no. 792, Apr. 6, 1929, pp. 440-465.
2. Theodorsen, Theodore: Theory of Propellers. McGraw-Hill Book Co., Inc., 1948.
3. Kuethe, Arnold M and Schetzler, J. D.: Foundations of Aerodynamics. John Wiley & Sons, Inc., 1950.
4. Sullivan, J. P.: The Effect of Blade Sweep on Propeller Performance AIAA Paper 77-716, June 1977.
5. Egolf, T. A.; et al.: An Analysis for High Speed Propeller-Nacelle Aerodynamic Performance Prediction. Vol. 1 - Theory and Initial Application. Vol. 2 - User's Manual for the Computer Program. R79-912949-19, United Technologies Research Center.
6. Chaussee, D. S.: Computation of Three-Dimensional Flow Through Prop Fans. NEAR-TR-169, Nielsen Engineering and Research, Inc., 1979.
7. Bober, L. J. and Mitchell, G. A.: Summary of Advanced Methods for Predicting High Speed Propeller Performance. AIAA Paper 80-0225, Jan. 1980; also NASA TM 81409, 1980.

## ESTABLISHED APPROACH

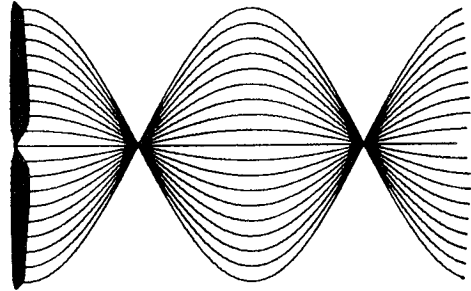
### MODEL

WAKE - RIGID HELICAL VORTEX SHEET

SINGLE OR COUNTER ROTATION

BLADES - STRAIGHT LIFTING LINE

NACELLE - NONE



### SOLUTION TECHNIQUE

STRIP ANALYSIS

CS-79-4089

Figure 1

## CURVED LIFTING LINE ANALYSIS

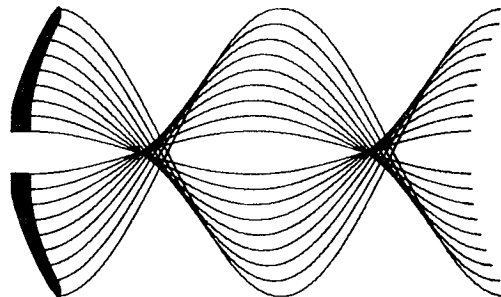
### MODEL

WAKE - RIGID HELICAL VORTEX FILAMENTS

SINGLE ROTATION

BLADES - CURVED LIFTING LINE

NACELLE - INFINITE CYLINDER



### SOLUTION TECHNIQUE

SIMULTANEOUS SOLUTION FOR BLADE

AND WAKE VORTEX STRENGTHS

CS-79-4088

Figure 2

## CURVED LIFTING LINE RESULTS

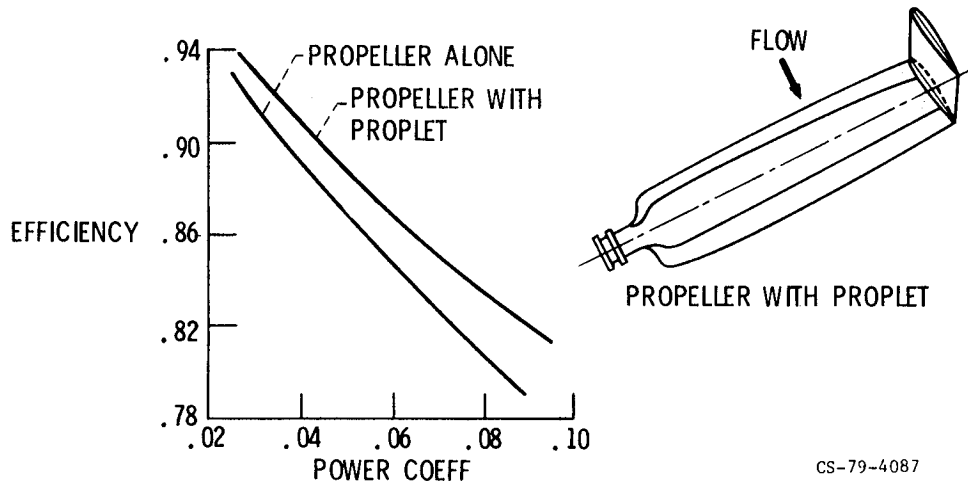


Figure 3

CS-79-4087

## PROPELLER NACELLE INTERACTION ANALYSIS

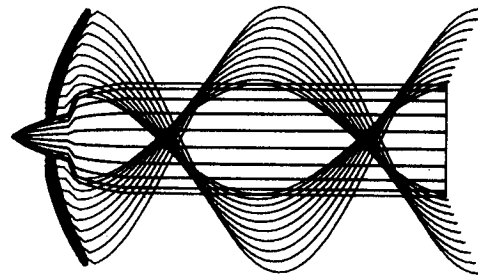
### MODEL

WAKE - VORTEX FILAMENTS ALONG  
STREAM SURFACES

SINGLE OR COUNTER  
ROTATION

BLADES - CURVED LIFTING LINE

NACELLE - ARBITRARY GEOMETRY



### SOLUTION TECHNIQUE

INVISCID NACELLE SOLUTION TO  
LOCATE WAKE FILAMENTS

INDUCED ANGLE OF ATTACK DUE  
TO WAKE

BLADE FORCES USED IN  
CIRCUMFERENTIALLY AVERAGED  
VISCOUS FLOW

CS-79-4090

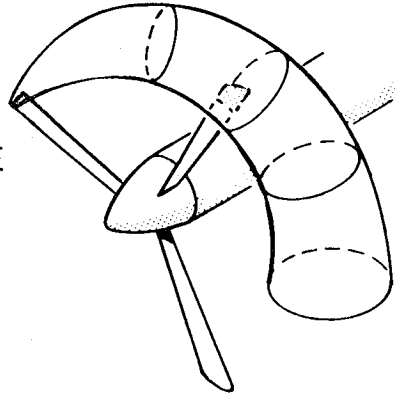
Figure 4

# HIGH SPEED EFFECTS

## PROPELLER NACELLE INTERACTION ANALYSIS

SUPERSONIC FLOW REGIONS OF INFLUENCE

SUPERSONIC TIP CORRECTION

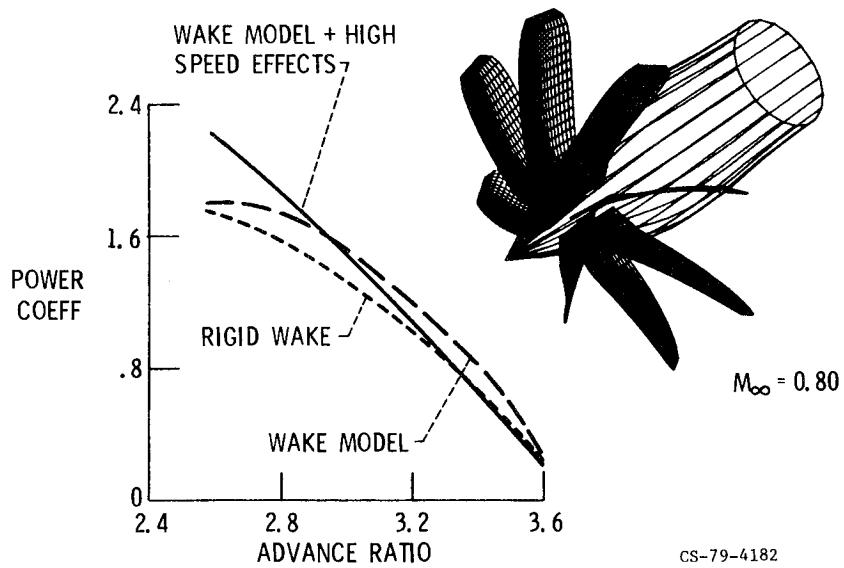


CS-79-3788

Figure 5

## EFFECT OF LIFTING LINE REFINEMENTS

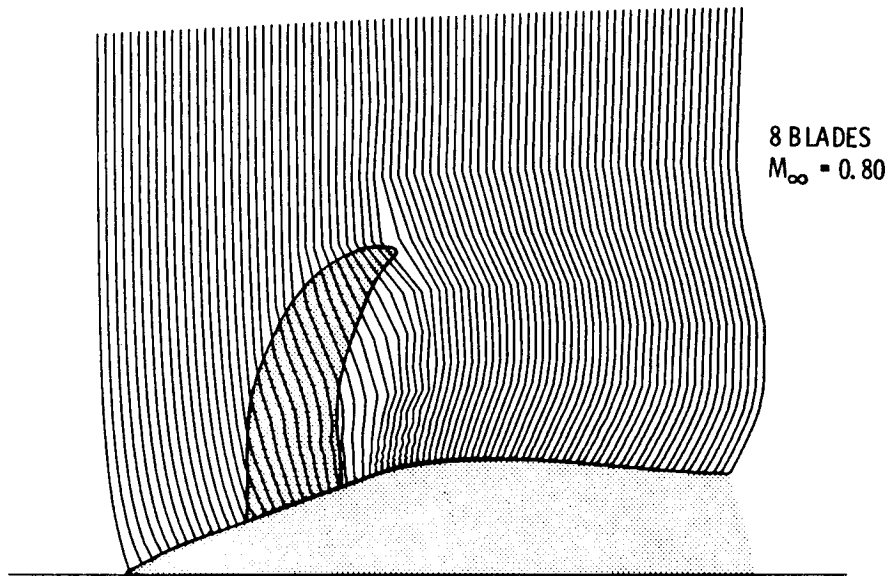
### PROPELLER NACELLE INTERACTION ANALYSIS



CS-79-4182

Figure 6

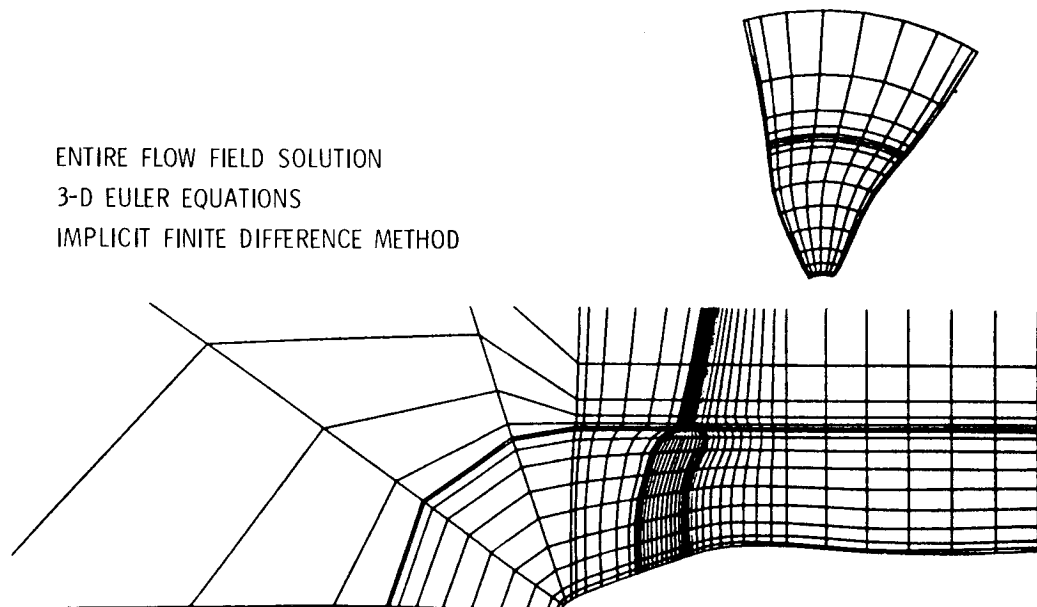
PROPELLER INDUCED SWIRL VELOCITIES  
PROPELLER NACELLE INTERACTION ANALYSIS



CS-79-3888

Figure 7

3-D COMPRESSIBLE LIFTING SURFACE ANALYSIS

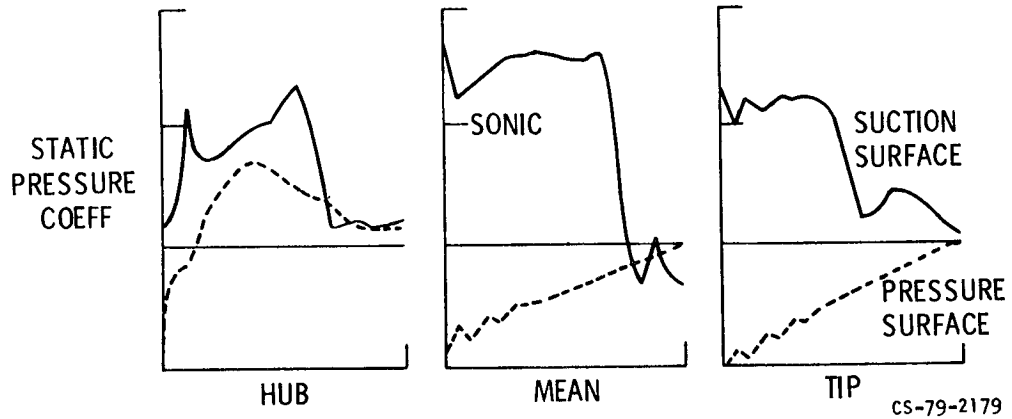


CS-79-4124

Figure 8

### 3-D COMPRESSIBLE LIFTING SURFACE RESULTS

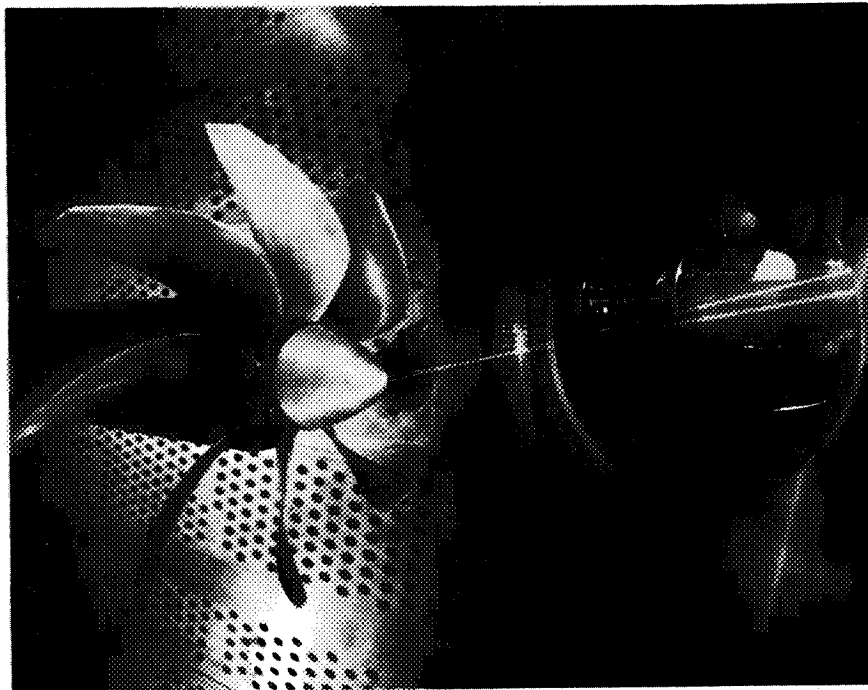
$$M_{\infty} = 0.8, M_{TIP} = 1.15$$



CS-79-2179

Figure 9

### LASER VELOCIMETER MEASUREMENTS



CS-79-3707

Figure 10

